© 2021. Published by The Company of Biologists Ltd | Journal of Experimental Biology (2021) 224, jeb242820. doi:10.1242/jeb.242820

RESEARCH ARTICLE

# Increased cellular detoxification, cytoskeletal activities and protein transport explain physiological stress in a lagoon sponge

**Sandeep S. Beepat*, Simon K. Davy, Clinton A. Oakley, Amirhossein Mashini, Lifeng Peng and James J. Bell**

## ABSTRACT

Tropical lagoon-inhabiting organisms live in highly irradiated ecosystems and are particularly susceptible to thermal stress resulting from climate change. However, despite living close to their thermal maxima, stress response mechanisms found in these organisms are poorly understood. We used a novel physiological–proteomic approach for sponges to describe the stress response mechanisms of the lagoon-inhabiting sponge *Amphimedon navalis*, when exposed to elevated seawater temperatures of +2°C and +4°C relative to a 26°C ambient temperature for 4 weeks. After 4 weeks of thermal exposure, the buoyant weight of the sponge experienced a significant decline, while its pumping rates and oxygen consumption rates significantly increased. Proteome dynamics revealed 50 differentially abundant proteins in sponges exposed to elevated temperature, suggesting that shifts in the sponge proteome were potential drivers of physiological dysfunction. Thermal stress promoted an increase in detoxification proteins, such as catalase, suggesting that an excess of reactive oxygen species in sponge cells was responsible for the significant increase in oxygen consumption. Elevated temperature also disrupted cellular growth and cell proliferation, promoting the loss of sponge biomass, and the high abundance of multiple α-tubulin chain proteins also indicated an increase in cytoskeletal activities within sponge cells, which may have induced the increase in sponge pumping rate. Our results show that sustained thermal exposure in susceptible lagoonal sponges may induce significant disruption of cellular homeostasis, leading to physiological dysfunction, and that a combined physiological–proteomic approach may provide new insights into physiological functions and cellular processes occurring in sponges.

**KEY WORDS: Sponge, Physiology, Proteomics, Thermal stress, Lagoon, Climate change**

## INTRODUCTION

Tropical coastal lagoons are highly productive semi-enclosed ecosystems that are important habitats for many marine organisms (Kennish and Paerl, 2010). However, given that coastal lagoons are generally high-irradiance ecosystems with shallow topography and low flushing rates, they may particularly be susceptible to heat accumulation (Kennish, 2016; Pérez-Ruzafa et al., 2019). For example, lagoon-inhabiting corals around tropical Pacific islands (Hoegh-Guldberg et al., 2011) and East Africa (McClanahan et al., 2007) have suffered significant bleaching when exposed to elevated temperatures. However, while the consequences of climate change on lagoon-inhabiting corals are well documented (McClanahan et al., 2007, 2011; Hoegh-Guldberg, 1999), the impacts of climate change on other non-conspicuous lagoon-inhabiting benthic taxa, such as sponges, are poorly understood.

Sponges are important functional components of marine ecosystems (Wulff, 2006; Bell, 2008) and are often important components of lagoonal benthic communities (Ilan and Abelson, 1995; Levi et al., 1998; Beepat et al., 2013). As a result of their efficient filtering capabilities (Reiswig, 1971), sponges provide an important link between the benthos and the water column (De Goeij et al., 2013; Rix et al., 2018) and they have an important role in nutrient cycling (Maldonado et al., 2012; De Goeij et al., 2017). In coastal lagoons, sponges have also been reported to act as substrate stabilizers (Cerrano et al., 2004; Wulff, 2016) and provide habitats for a suite of macrofaunal invertebrates (Beepat et al., 2014; Ávila and Ortega-Bastida, 2015). Despite their ecological importance, the impacts of climate change on lagoon-inhabiting sponges are relatively undescribed. Therefore, understanding stress response mechanisms in lagoon-inhabiting sponges may provide important insights into the physiology and functional cellular processes occurring in non-motile lagoonal benthic communities exposed to anthropogenic stressors.

The effects of elevated temperature on sponge physiology are thought to be species specific (see review by Bell et al., 2018). While some sponges, such as *Cliona celata* (Miller et al., 2010; Duckworth and Peterson, 2013) and *Aplysina cauliformis* (Duckworth et al., 2012), are known to be tolerant of moderate elevated temperatures, other species are less tolerant to thermal increases (Bell et al., 2018). For example, the sponge *Rhopaloeides odorabile* experienced reduced pumping and filtration rates when exposed to an increase of 3°C for 16 days (Massaro et al., 2012). Extensive bleaching and lower bioerosion rates were also reported for *Cliona orientalis* exposed to an increase of 2.7°C above maximum monthly mean temperatures for 10 weeks (Achlatis et al., 2017). However, while sponge physiological responses to elevated temperature have been well described, the molecular responses of thermally treated sponges have been relatively poorly studied (Pantile and Webster, 2011; Webster et al., 2013).

To date, thermally induced molecular responses in sponges have mostly been documented in the reef sponge *R. odorabile* (Pantile and Webster, 2011; Fan et al., 2013; Webster et al., 2013). Changes in gene expression, including actin (cytoskeletal arrangements), ubiquitin conjugating enzyme, elongation factor-Tu (protein synthesis/degradation), calmodulin, (signal transduction) and ferritin (oxidative stress) were reported after a thermal exposure of 0.5–2°C for 3 days (Pantile and Webster, 2011; Webster et al., 2013). Similarly, the induction of multiple genes involved in signal transduction and immunity pathways were reported from the sponge

School of Biological Sciences, Victoria University of Wellington, Wellington 6140, New Zealand.

*Author for correspondence (sandeep.beepat@vuw.ac.nz)

S.S.B., 0000-0002-0224-4776; S.K.D., 0000-0003-3584-5356; C.A.O., 0000-0002-4673-0645; A.M., 0000-0003-3898-4968; L.P., 0000-0002-2043-5912; J.J.B., 0000-0001-9996-945X

**Received 4 May 2021; Accepted 13 October 2021**

*Halicona tubifera* when exposed to increasing temperatures of +3°C and +5°C, respectively (Guzman and Conaco, 2016). Increased expression in Hsp70 gene has also been reported in thermally stressed *Geodia cydonium* (Krasko et al., 1997) and *Xestospongia muta* (López-Legentil et al., 2008). While molecular stress responses in sponges have mainly been tested using gene expression (Webster et al., 2013; Guzman and Conaco, 2016), no attempt has been made to explore the response mechanisms of sponges using proteomics.

Proteins are generally more stable than mRNAs (Eden et al., 2011; Vogel and Marcotte, 2012) and proteome dynamics can complement genomic approaches to enhance our understanding on the functional behaviours of an organism (Tyers and Mann, 2003; Cho, 2007). Such approaches can potentially provide novel information on the functional behaviour of the host's physiology or symbiont communities in response to environmental change (Liu et al., 2012). For example, proteome abundance patterns from the model symbiotic cnidarian *Exaiptasia pallida* revealed broad disturbances in protein folding and increased cellular stress from elevated temperature (Oakley et al., 2017). Recently, using a combined physiological–proteomic approach, Tisthammer et al., 2021 revealed potential underlying adaptative processes in the coral *Porites lobata.* While significant physiological changes and an increase in proteins involved in detoxification, antioxidant defense and regulation of metabolic processes were reported in offshore *P. lobata* populations, no significant changes in physiological responses and proteome dynamics were seen in nearshore-inhabiting populations, suggesting that nearshore benthic organisms may be more resilient to anthropogenic stressors. In sponges, aerobic nitrification, and transportation and degradation of halogenated compounds have previously been reported for the microbiomes of the sponges *Cymbastela concentrica* (Liu et al., 2012) and *Aplysina aerophoba* (Chaib De Mares et al., 2018), using metaproteomic approaches. Given that lagoon-inhabiting benthic communities are directly exposed to elevated temperatures, a combined physiological–proteomic approach may enhance our understanding on the potential underlying cellular mechanisms occurring in these organisms.

The sponge *Amphimedon navalis* is a common species found in the shallow coastal lagoons of Mauritius in the western Indian Ocean (Beedessee et al., 2012; Beepat, 2015) and along the East African coast (Pulitzer-Finali, 1993). While this species may be tolerant to excess nutrients, it has been reported to experience significant loss in mass and increased respiration rates when exposed to an elevated sweater temperature of +4°C, which can lead to mortality (Beepat et al., 2020). Here, we investigate the physiological and proteomic responses of this lagoon-inhabiting sponge when exposed to temperatures of +2°C and +4°C (IPCC, 2014) above the ambient seawater temperature (26°C) over a period of 4 weeks. We hypothesize that *A. navalis* will experience significant physiological and cellular stress when exposed to elevated temperatures. Changes in buoyant weight, oxygen consumption and sponge pumping rates were measured weekly, and the protein dynamics of *A. navalis* were assessed after 4 weeks to identify any potential cellular mechanisms that may be involved in thermally susceptible sponges.

## MATERIALS AND METHODS

### Sponge collection

Specimens of the sponge *Amphimedon navalis* Pulitzer-Finali 1993, ranging in size from 4 to 10 cm, were collected from the lagoon of Trou D'eau Douce, Mauritius (20°14′ S, 57°47′ E) at a depth of 0.5–1 m. Approximately 45 min after collection, sponges were transported to a laboratory facility and transferred to 10-liter tanks of freshly collected seawater at an ambient temperature of 26°C (average seawater temperature at collection sites). Light conditions in the laboratory facility were maintained at a maximum irradiance of approximately 450 µmol photons $m^{-2}$ $s^{-1}$, which corresponds to the irradiance at a depth of 0.5 m at the collection site. Photosynthetically active radiation in the laboratory was monitored using a pulse amplitude modulated fluorometer (red LED Diving PAM, Walz, Germany).

### Experimental design

The thermal experiment was conducted in summer (December 2018). Experimental tanks were supplied with individual 100 W aquarium heaters and were aerated using aquarium oxygen pumps. Food supply for sponges was maintained by manually replacing unfiltered freshly collected seawater at 12-h intervals, based on prior sponge pumping rate calculations. Sponge pumping rates were estimated to determine the volume of water that sponges would recycle per day, ensuring that seawater in the tanks was re-circulated no more than three times through the sponges (Beepat et al., 2020). Sponges were acclimatized for 1 week (the acclimation week) prior to the start of the temperature-stress experiment. Sponges were then transferred to pre-heated treatment tanks. A 4-week thermal exposure period was scheduled. The total length of the experiment was 5 weeks including the acclimation week.

Three temperature treatments (26, 28 and 30°C, range±0.5°C) were chosen based on the IPCC (2014) SST prediction scenarios for 2100 using the Representative concentration pathways RCP6.0 (+2°C) and RCP8.5 (+4°C) relative to the current ambient seawater temperature in Mauritius (26°C) during the summer (Turner et al., 2000; Fagoonee, 1990). The experimental design consisted of a total of nine treatment tanks (i.e. three replicate tanks for each temperature treatment) with a holding capacity of 10 liters, with each tank containing 5 sponges. Three sponges from each tank ($n$=9 per temperature treatment) were exclusively used to assess physiological changes over time. The remaining two sponges ($n$=6 per temperature treatment) were sacrificed at the end of the experiment for proteome dynamics. Three 20-liter tanks were used to pre-heat seawater daily and pre-heated seawater was manually replaced at 12-h intervals. Temperature data loggers (Onset, Hobo, MA, USA) were used to monitor temperature fluctuations in the treatment tanks at 3-h intervals (Fig. S1). Sponge survival and health were monitored daily and sponges showing any signs of disease (necrosis or formation of white film) were immediately removed (Bennett et al., 2017; Bates and Bell, 2018). Physiological responses were measured at weekly time-points (T0, T1, T2, T3 and T4) for 4 weeks after the acclimation week.

### Physiological responses

#### Buoyant weight

The buoyant weight of each sponge was measured weekly following the methods of Osinga et al. (1999) using a digital scale (Scout STX422, Ohaus, USA).

#### Holobiont oxygen consumption

Holobiont (sponge+symbionts) oxygen consumption was measured in cylindrical 100 ml acrylic closed respiration chambers following the methods described in Beepat et al. (2020), using a dissolved oxygen meter (PreSens, Fibrox 3, Germany) under ambient light

conditions (430–450 µmol photons $m^{-2}$ $s^{-1}$). Static respirometry was used to assess sponge oxygen consumption rates. To control for any electrode drift resulting from free-floating micro-organisms, oxygen concentration levels were also measured in an empty respiration chamber containing seawater. Respiration chamber temperature was regulated by a water bath and oxygen consumption rate was recorded across a total of 30 min following an incubation period of 5–10 min. Measurements were ended prematurely if the oxygen concentration fell below 70% of the original concentration (100%), to reduce any anoxic stress to the sponge (Biggerstaff et al., 2015). Oxygen consumption measurements were standardized to sponge ash-free dry weight using the conversion ratio of 0.39±0.04 (Beepat et al., 2020).

#### Sponge pumping rate

Sponge pumping rates were measured following the methods of Massaro et al. (2012). A ruler was vertically attached to the bottom of a transparent 2-liter glass beaker and the target sponge was carefully transferred into the beaker with the osculum facing upwards. Approximately 1 ml fluorescein dye was carefully released at the base of the sponge using a syringe and the exhaled dye movement from the sponge's osculum was recorded. In situations where the sponge's osculum could not be placed facing upwards in the beaker (e.g. the sponge osculum was horizontal), the glass beaker was placed on graph paper and the exhaled horizontal movement of the dye was recorded on video from the top of the beaker and analyzed. The pumping rate was calculated by measuring the time taken for the fluorescein dye to travel a known distance from the osculum opening to a specific point on the ruler/graph paper. Pumping rate (ml $s^{-1}$) was then multiplied with the cross-sectional area of the sponge's osculum.

### Proteomic responses

#### Protein extraction

At the end of the thermal experiment (T4), *A. navalis* sponges ($n$=6 per treatment; two sponges from each tank) were frozen at −20°C for proteome analysis. Prior to peptide extraction, sponge samples were kept overnight in 99.5% ethanol at −20°C to remove any excess pigments associated with the sponge (Sproles et al., 2019). Peptides were prepared using a sodium deoxycholate (SDC) in-solution digestion method modified from Oakley et al. (2016). Sponge samples were homogenized for 30 s using a tissue homogenizer (Thermo Fisher Scientific Inc., USA) and incubated at 85°C for 20 min in 5% SDC, followed by adding 1% β-mercaptoethanol (BME) to the solution to denature proteins. SDC and residual pigments were extracted from the solution via ethyl acetate phase transfer (Yeung and Stanley, 2010) and cell debris was removed by centrifugation at 10,000 ***g*** for 2 min. Lysates were processed using a modified method of the filter-aided sample preparation from Wiśniewski et al. (2009). Lysates were transferred to 0.5 ml Amicon Ultra centrifugal units (Sigma-Aldrich, MO, USA), centrifuged at 14,000 ***g*** for 15 min, mixed with 380 µl of 50 mmol $l^{-1}$ Tris buffer and centrifuged again. A subsample of 100 µg was alkylated using 50 mmol $l^{-1}$ acrylamide, incubated at room temperature for 20 min and digested with 2 µg trypsin at 37°C for 12-18 h. Formic acid (0.1% final) was added to terminate trypsin digestion and precipitate any remaining SDC. The peptide solution was centrifuged at 16,000 ***g*** for 2 min to pellet the SDC precipitate. Peptides were then desalted using 50% and 30% acetonitrile and resuspended in 0.1% formic acid at 37°C for 30 min. Protein and peptide concentrations were assessed by bound dye fluorescence (Qubit, Thermo Fisher Scientific Inc., USA).

#### Liquid chromatography-tandem mass spectrometry

Peptide separation was conducted on an Acclaim PepMap C18 column (Thermo Fisher Scientific, Auckland, New Zealand) and a liquid chromatogram system (Ultimate 3000, Dionex, Sunnyvale, CA), using a 75 min linear gradient from 5% to 35% buffer B (buffer A: 0.1% formic acid; buffer B: 80% acetonitrile, 0.1% formic acid) at 300 nl $min^{-1}$. Peptide ionization was conducted by 1.8 kV electrospray and acquired using an Orbitrap Fusion Lumos Tribrid mass spectrometer (Thermo Fisher Scientific). The acquisition of precursor mass spectra was performed using the following specifications: 120,000 resolution, rejecting single-charged ions, enabled quadrupole isolation with an automatic gain target of 700,000 and maximum injection time of 50 ms. Higher-energy collision dissociation was used to fragment the 20 most intense precursor spectra and analysis was performed in the ion trap (automatic gain target and maximum injection time set at 5000 and 300 ms, respectively).

#### Protein identification and quantification

The Andromeda search algorithm in MaxQuant was used for protein identification (Cox et al., 2014) against the genome of the sponge *Amphimedon queenslandica* (Srivastava et al., 2010) in UniProtKB (https://www.uniprot.org/). Trypsin digestion with a maximum of two missed cleavages was assumed. The carbamidomethylation of cysteine was assumed as a fixed modification, and oxidation of methionine and acetylation of the protein N-terminus set as variable modifications. Peptide tolerances for first and main searches were 20 ppm and 4.5 ppm, respectively, and for ion trap MS2 search, a mass tolerance of 0.5 Da was used. Protein quantification was conducted using label-free quantification. Searches were performed with a false discovery rate (FDR) of 2.5% and a minimum of two peptides per protein were required for identification. Protein annotations were matched using the web-based tool QuickGo (Binns et al., 2009) in UniProtKB. The mass spectrometry data are available from the PRIDE repository (Perez-Riverol et al., 2019) with the identifier PXD027246.

### Data analysis

Statistical analyses for physiological responses were performed using SPSS v.24 (SPSS Statistics for Windows, IBM Inc, NY, USA). General Linear Mixed Models (GLMMs) were used to test the fixed effects of time and temperature on the sponges' physiological response. To account for pseudo-replication (nested design), all models were fitted with sponge replicates and tanks as random effects. Physiological response data were log ($x$+1) transformed. For each model, *post hoc* pairwise comparisons with Šídák applied correction were conducted to assess significant differences between the treatments at each time-point (see Table S1). Proteomic label-free quantification data were analyzed using PolySTest (Schwämmle et al., 2020) and the bioinformatics software Perseus v.1.6.13.0 (Tyanova and Cox, 2018). Known contaminant proteins and known false identification were filtered and label-free quantification data for the remaining proteins $\log_2$-transformed. Principal components analysis (PCA) plots were constructed using the filtered $\log_2$-transformed database. The Miss test (Schwämmle et al., 2020) was used to assess the effects of elevated temperature on *A. navalis* protein abundance while accounting for missing protein data points in some samples. An FDR threshold of 0.1 and log-ratio thresholds of ±0.25 were used to defined statistically significant proteins (see Table S2).

Journal of Experimental Biology (2021) 224, jeb242820. doi:10.1242/jeb.242820

## RESULTS

### Physiological responses

*Amphimedon navalis* buoyant weight significantly decreased with elevated temperature ($F_{2,68}$=43.652, $P$<0.001) and over time ($F_{8,68}$=28.199, $P$<0.001; Fig. 1A). After 4 weeks, *A. navalis* buoyant weight declined between 0.77–2.33% at 28°C, and 1.22–5.33% at 30°C. However, in the control treatment, the buoyant weight of this species increased by 0.83–2.33% over the same period. Buoyant weight was significantly lower in all higher temperature treatments relative to the controls ($P$<0.05; Table S1).

Oxygen consumption rate significantly increased with elevated temperature ($F_{2,75}$=5.958, $P$<0.001) and across time ($F_{8,75}$=47.904, $P$<0.001; Fig. 1B). *A. navalis* oxygen consumption rate after 4 weeks was 0.089–0.121 $O_2$ $g^{-1}$ $min^{-1}$ for the control, 0.110–0.145 $O_2$ $g^{-1}$ $min^{-1}$ at 28°C and 0.139–0.204 $O_2$ $g^{-1}$ $min^{-1}$ at 30°C. Oxygen consumption for this species was significantly higher at 28°C and 30°C versus 26°C ($P$<0.05; Table S1).

Sponge pumping rate significantly increased with elevated temperature ($F_{2,73}$=38.366, $P$<0.001) and over time ($F_{8,73}$=45.396, $P$<0.001; Fig. 1C). Pumping rate at T4 was 0.070-0.120 ml $s^{-1}$ at the control temperature, 0.150–0.180 ml $s^{-1}$ at 28°C and 0.160–0.230 ml $s^{-1}$ at 30°C. Sponge pumping rate was significantly higher at both elevated temperatures relative to the control ($P$<0.05; Table S1).

### Proteomic responses

#### Protein dynamics

*Amphimedon navalis* proteomic analysis yielded a total of 814 identified proteins. The most abundant proteins were representative of cellular compartments such as the cytoskeleton/microtubules, membrane, ribosome, and nucleosome. The molecular and biological functions of the 25 most abundant proteins based on their respective Gene Ontology (GO) annotations are described in Table 1.

#### Effect of temperature on protein dynamics

Of the 814 identified proteins, 50 were differentially abundant when exposed to elevated temperature (FDR<0.1). PCA analysis revealed that similarities between protein abundances were mostly grouped among temperature treatments, except for sponges exposed to 30°C, where three samples were significantly dispersed (Fig. S2). 72% of the differentially abundant proteins (36 proteins) were significantly enriched while the remaining 28% were significantly less abundant at increased temperature conditions (Table 2). Protein enrichment was mostly found for proteins involved in cytoskeletal organization, oxidative stress and protein translation. In contrast, significant decline was mostly apparent for proteins involved in transportation and protein catabolism. Of the 50 differentially abundant proteins, 10 (listed as ‘others’) were uncharacterized with no GO annotation.

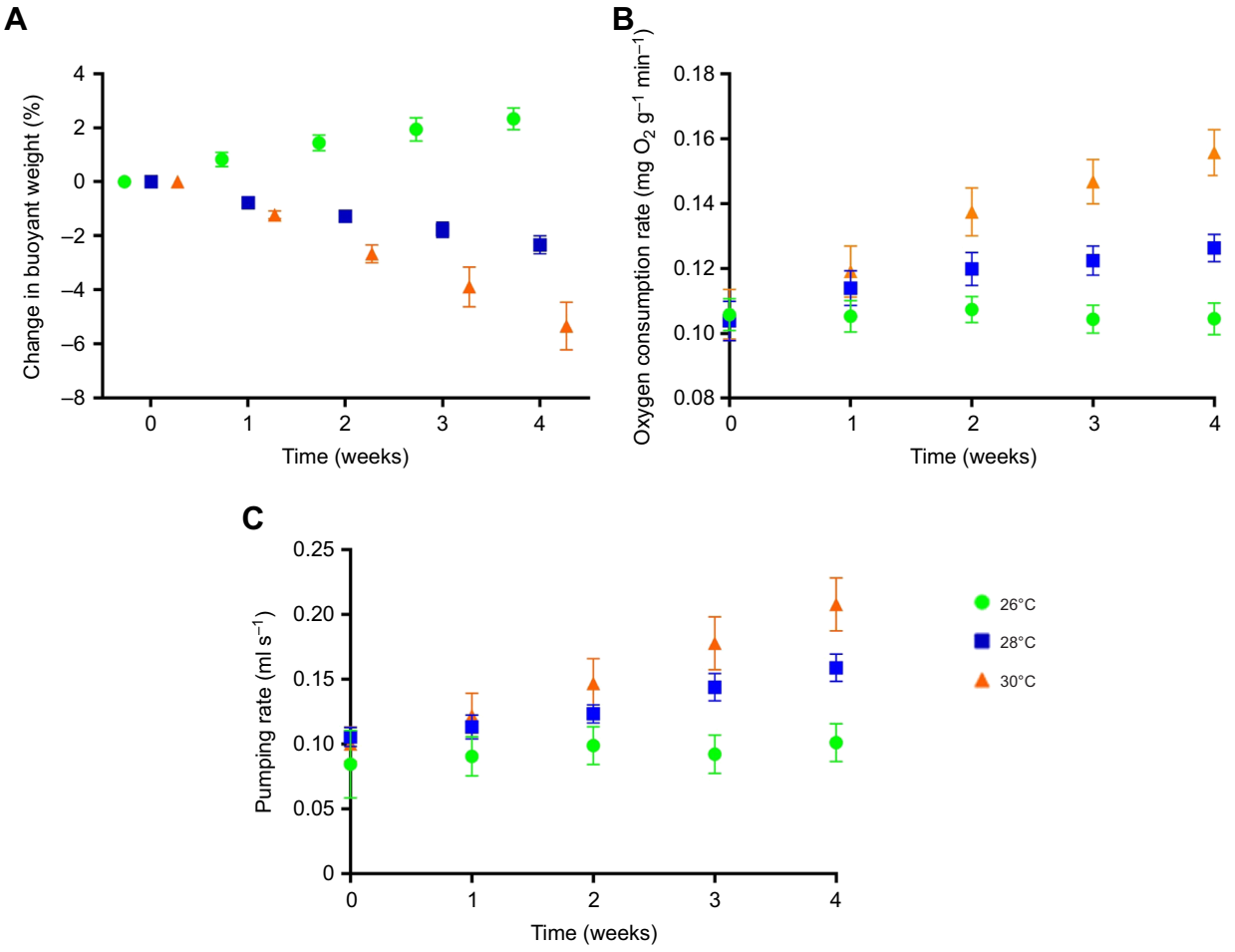


**Fig. 1. Percentage change in buoyant weight, oxygen consumption and pumping rate of *Amphimedon navalis* in response to elevated temperature.** Values are means±s.e.m. at each time point after 4 weeks at 26, 28 or 30°C ($n$=9 per treatment per time point). Holobiont oxygen consumption values are mean per gram of sponge ash free dry weight.



Journal of Experimental Biology

**Table 1. Twenty-five most abundant proteins detected from the marine sponge *Amphimedon navalis* after a 4-week exposure to different temperatures as estimated by label-free quantification**

| UniProtKB accession number | Protein annotation | Molecular function | Biological process |
|---|---|---|---|
| A0A1X7VST2 | Uncharacterized (Actin family) | ATP binding | Cytoskeletal organization |
| A0A1X7VM44 | Tubulin β-chain | GTP and nucleotide binding | Cytoskeletal organization |
| A0A1X7U5Q4 | Uncharacterized (Gelsolin-like domain protein) | Actin filament binding | Cytoskeletal organization |
| A0A1X7VHU9 | NAD(P)H oxidase ($H_2O_2$ forming) | Calcium and heme binding/oxidoreductase activity | Oxidation-reduction process |
| A0A1X7UUJ9 | 40S ribosomal protein S8 | Structural constituent of ribosome | Translation |
| A0A1X7V9A9 | Clathrin heavy chain | Clathrin light chain binding | Protein transport |
| A0A1X7VLR9 | Histone H4 | DNA binding | DNA-template transcription |
| A0A1X7UXJ8 | Uncharacterized (α-actinin family) | Calcium and actin ion binding | Cytoskeletal organization |
| A0A1X7VL10 | ATP synthase subunit β | ATP and nucleotide binding | Proton transport |
| A0A1X7T260 | Histone H2A | DNA binding | DNA folding |
| A0A1X7V9W5 | HATPase_c domain-containing protein | ATP and nucleotide binding | Protein folding |
| A0A1X7V3W4 | Uncharacterized (HSP70 family) | ATP and nucleotide binding | Protein folding |
| A0A1X7VSH2 | Uncharacterized (Myosin family) | Actin and ATP binding/Motor activity | Cytoskeletal organization |
| A0A1X7VNW3 | Catalase | Heme and metal ion binding | Oxidation-reduction process |
| A0A1X7VRP4 | Histone domain-containing protein (Histone 2B family) | DNA binding | DNA folding |
| A0A1X7VAN2 | Calmodulin | Calcium and metal ion binding | Calcium-mediated signaling |
| A0A1X7V1A0 | Uncharacterized protein (HSP60 family) | ATP and nucleotide binding | Protein folding |
| A0A1X7V0I1 | 60S ribosomal protein L40 | Structural constituent of ribosome | Translation |
| A0A1X7UPB4 | Tubulin α-chain | GTP binding | Cytoskeletal organization |
| A0A1X7TRT9 | Uncharacterized | – | – |
| A0A1X7UQ10 | Tubulin α-chain | GTP and nucleotide binding | Cytoskeletal organization |
| A0A1X7UKV7 | Uncharacterized (mitochondrial carrier family) | Transmembrane transporter activity | Protein transport |
| A0A1X7V5G1 | Uncharacterized | GTP binding | – |
| A0A1X7UIL6 | Uncharacterized (ATPase α/β- chain family) | ATP and nucleotide binding/proton-transporting ATP synthase activity (rotational mechanism) | Proton transport |
| A0A1X7VWH7 | ADF-H domain-containing protein | Actin binding | Cytoskeletal organization |

The Miss test revealed that differences in protein abundance were most pronounced in sponges exposed to 30°C relative to the controls, where 43 proteins were differentially abundant (33▲ and 10▼) at the end of the experiment. For sponges exposed to 28°C, 25 proteins were differentially abundant in comparison to the controls. Seventeen proteins were significantly more abundant, and 8 proteins experienced significant decline. On the other hand, 15 proteins were differentially abundant at 30°C relative to 28°C, of which 11 were enriched and the abundance of 4 proteins significantly declined (Fig. 2). Tubulin α-chain, calmodulin, proteasome subunit β and adenosylhomocysteinase were significantly more abundant, whereas the abundances of uncharacterized (ABC transporter-like family) and sulfatase domain-containing proteins declined significantly between all comparative treatments (Fig. 3).

## DISCUSSION

Tropical lagoon-inhabiting organisms are directly exposed to elevated temperatures and probably live near to their thermal tolerance limit (Anthony et al., 2009). However, stress response mechanisms in lagoon-inhabiting sponges are poorly understood. Here, we assessed a combination of physiological and proteomic responses in the thermally susceptible lagoon-inhabiting sponge *Amphimedon navalis*, to identify potential stress response mechanisms. While *A. navalis* buoyant weight declined significantly as a result of thermal exposure, its pumping and oxygen consumption (i.e. respiration) rates increased significantly over time. These observations are indicative of increased metabolic cost and thermal stress (Leys et al., 2011; Massaro et al., 2012; Fang et al., 2014). Proteome dynamics revealed that 50 proteins, which are mostly involved in oxidation/reduction, protein transport and cytoskeletal organization processes, were differentially abundant after 4 weeks of thermal exposure. While most of the differentially abundant proteins were significantly more abundant in sponges exposed to elevated temperature, some proteins, such as ATP synthase subunit β (protein transport) and sulfatase domain-containing protein (protein catabolism), were significantly less abundant. These observations demonstrate that the lagoon sponge *A. navalis* is significantly susceptible to elevated temperatures, supporting the initial findings of Beepat et al. (2020). Induced thermal stress resulted in considerable cellular dysfunction leading to increased detoxification processes, cytoskeletal activities and protein folding, resulting in the loss of sponge biomass, and increased respiration and pumping rates.

Stress response mechanisms in response to thermal exposure have previously been reported for reef (López-Legentil et al., 2008; Pantile and Webster, 2011; Webster et al., 2013), temperate (Koutsouveli et al., 2020) and Antarctic (González-Aravena et al., 2019) sponges. Pantile and Webster (2011) and Webster et al. (2013) demonstrated that the reef sponge *R. odorabile* experienced significant downregulation in multiple genes involved in protein folding and cytoskeletal arrangement when exposed to elevated temperatures of up to +5°C for 15 days. Guzman and Conaco (2016) also showed that a 3-day thermal exposure of up to +5°C increased the expression of heat shock proteins, antioxidants and genes involved in signal transduction in the sponge *Haliclona tubifera*. Recently, Koutsouveli et al. (2020) demonstrated that the sponge *Spongia officinalis* experienced major transcriptomic shifts in response to elevated temperatures, which triggered processes related to signal transduction, inflammation and apoptotic pathways. While these studies were able to determine potential stress responses from marine sponges, they were based on mRNA transcript counts, which often do not correlate well with protein abundance (Vogel and Marcotte, 2012). The present study therefore demonstrates the utility of proteomics in linking physiology to the proteome more

Journal of Experimental Biology (2021) 224, jeb242820. doi:10.1242/jeb.242820

**Table 2. Differentially abundant proteins (FDR<0.1, ±0.25-fold change) from the marine sponge *Amphimedon navalis* after a 4-week exposure to different temperatures**

| UniProtKB accession number | Protein annotation | Proteins in cluster | Log-ratio 26°C vs. 28°C | Log-ratio 26°C vs. 30°C | Log-ratio 28°C vs. 30°C | No. of unique peptides |
|---|---|---|---|---|---|---|
| **Oxidation-reduction process (Oxidative stress)** | | | | | | |
| A0A1X7V4C4 | Aldedh domain-containing protein | 2 | 2.42 ▲ | 0.71 ▲ | –1.70 | 3 |
| I1GFQ7 | Ferritin | 2 | 2.40 ▲ | 2.05 ▲ | –0.34 | 4 |
| A0A1X7SUN1 | VOC domain-containing protein | 2 | 0.94 | 1.54 ▲ | 0.59 | 2 |
| A0A1X7VNW3 | Catalase (Heme cofactor) | 2 | 0.62 | 0.92 ▲ | 0.30 ▲ | 7 |
| A0A1X7VQL2 | Uncharacterized (Thioredoxin-like superfamily) | 1 | 0.32 | 2.00 ▲ | 1.68 ▲ | 1 |
| A0A1X7UNX4 | Uncharacterized (Glutathione S-transferase superfamily) | 1 | –0.23 | 3.31 | 3.54 ▲ | 1 |
| A0A1X7T3Q9 | E1_dh domain-containing protein | 2 | –0.41 | 1.98 ▲ | 2.39 ▲ | 2 |
| A0A1X7VJL6 | Peroxiredoxin | 1 | –1.34 | –2.51 ▼ | –1.16 | 2 |
| A0A1X7U633 | Cytochrome *c* domain-containing protein | 2 | –2.35 | –4.19 ▼ | –1.83 ▼ | 3 |
| A0A1X7V4Y0 | Proton-translocating NAD(P) (+) transhydrogenase | 1 | –2.37 ▼ | –2.01 ▼ | 0.36 | 8 |
| **Protein transport** | | | | | | |
| A0A1X7U4A4 | Protein kinase domain-containing protein | 1 | 1.51 ▲ | 1.50 ▲ | –0.01 | 1 |
| A0A1X7UVI1 | Protein kinase domain-containing protein | 1 | 1.13 | 1.82 ▲ | 0.69 | 3 |
| A0A1X7VH72 | Uncharacterized (inositol phosphokinase family) | 1 | 0.84 ▲ | 1.11 ▲ | 0.27 | 2 |
| A0A1X7V114 | Vacuolar protein sorting-associated protein 11 homolog | 1 | 0.70 | 1.47 ▲ | 0.77 | 3 |
| A0A1X7UHM1 | Ras-related protein Rab-14 | 1 | 0.36 | 0.50 ▲ | 0.13 | 6 |
| A0A1X7VLI5 | Protein kinase domain-containing protein | 1 | 0.16 | 2.16 ▲ | 2.00 ▲ | 1 |
| A0A1X7VL10 | ATP synthase subunit β | 1 | –0.48 ▼ | –0.39 | 0.09 | 14 |
| A0A1X7VVN1 | Uncharacterized (ABC transporter-like family) | 1 | –0.82 ▼ | –1.26 ▼ | –0.43 ▼ | 0 |
| A0A1X7VJC1 | Uncharacterized (DUOXA family) | 1 | –2.98 ▼ | –1.99 | 0.98 | 2 |
| A0A1X7VXP7 | Uncharacterized (SNF7 family) | 1 | –3.35 ▼ | –3.93 ▼ | –0.57 | 2 |
| **Cytoskeletal organization** | | | | | | |
| A0A1X7UKK7 | Costars domain-containing protein | 1 | 4.11 ▲ | 3.33 ▲ | –0.78 | 2 |
| A0A1X7VU79 | Fascin | 1 | 3.20 ▲ | 0.62 | –2.58 | 3 |
| A0A1X7UPB4 | Tubulin α-chain | 1 | 1.31 ▲ | 3.80 ▲ | 2.48 | 2 |
| A0A1X7UIF6 | F-actin-capping protein subunit β | 1 | 0.78 | 0.36 | –0.41 ▼ | 5 |
| A0A1X7V1D4 | Tubulin α-chain | 1 | 0.52 ▲ | 1.11 ▲ | 0.59 ▲ | 3 |
| A0A1X7U6V8 | Septin-type G domain-containing protein | 2 | 0.50 ▲ | 0.04 | 0.55 ▲ | 6 |
| A0A1X7VTE3 | Uncharacterized (small GTPase family) | 1 | 0.48 | 0.46 ▲ | –0.02 | 9 |
| A0A1X7UXJ8 | Uncharacterized (α-actinin family) | 1 | 0.46 ▲ | 0.45 ▲ | –0.01 | 20 |
| A0A1X7V9U2 | Uncharacterized (WASH complex, subunit strumpellin) | 1 | 0.34 | 1.99 ▲ | 1.64 ▲ | 2 |
| A0A1X7U0F7 | PDZ domain-containing protein | 1 | –1.04 | –1.38 ▼ | –0.34 | 2 |
| **Signal transduction** | | | | | | |
| A0A1X7VAN2 | Calmodulin | 3 | 0.50 ▲ | 1.18 ▲ | 0.68 ▲ | 3 |
| A0A1X7UI48 | Histidine-tRNA ligase | 1 | –0.78 ▼ | –2.94 ▼ | –2.16 | 3 |
| A0A1X7VIG0 | ADP-ribosylation factor 6 (Arf family) | 1 | –2.51 | –2.82 ▼ | –0.30 | 3 |
| **Protein translation** | | | | | | |
| A0A1X7VB92 | Aspartate-tRNA ligase, cytoplasmic | 1 | 2.05 ▲ | 2.88 ▲ | 0.83 | 3 |
| A0A1X7V8E5 | Uncharacterized (Universal ribosomal protein S8 family) | 1 | 1.59 | 4.70 ▲ | 3.10 | 3 |
| A0A1X7V0I1 | Ubiquitin – 60S ribosomal protein L40 | 6 | 0.82 ▲ | 1.00 ▲ | 0.18 | 5 |
| **Protein catabolism** | | | | | | |
| A0A1X7VN30 | Proteasome subunit β | 2 | 3.04 ▲ | 4.96 ▲ | 1.92 ▲ | 2 |
| A0A1X7VGM8 | Palmitoyl-protein hydrolase 1 | 1 | –1.55 ▼ | –1.53 | 0.02 | 8 |
| A0A1X7VV07 | Sulfatase domain-containing protein ($Ca^{2+}$ cofactor) | 1 | –2.02 ▼ | –2.96 ▼ | –0.93 ▼ | 0 |
| **Metabolic process** | | | | | | |
| A0A1X7VEB3 | Adenosylhomocysteinase ($NAD^{+}$ cofactor) | 1 | 1.24 ▲ | 4.48 ▲ | 3.24 ▲ | 4 |
| **Others** | | | | | | |
| A0A1X7SVR6 | Uncharacterized | 4 | 3.77 ▲ | 5.15 ▲ | 1.38 | 1 |
| A0A1X7VMX7 | Septin-type G domain containing protein | 1 | 2.15 | 4.16 ▲ | 2.01 | 2 |
| A0A1X7SMT9 | Uncharacterized | 1 | 1.02 ▲ | 1.78 ▲ | 0.76 | 1 |
| A0A1X7VLW9 | Transket_pyr domain-containing protein ($Co^{2+}$ and $Mg^{2+}$ cofactor) | 1 | 0.88 | 0.40 ▲ | –0.48 | 4 |
| A0A1X7V015 | DUF3504 domain-containing protein | 1 | 0.86 | 2.32 ▲ | 1.46 | 1 |
| A0A1X7SJZ1 | Uncharacterized | 3 | 0.62 | 1.25 ▲ | 0.63 | 1 |
| A0A1X7SYB4 | Uncharacterized | 1 | 0.61 | 1.55 ▲ | 0.94 | 1 |
| A0A1X7U869 | Store-operated calcium entry-associated regulatory factor | 1 | 0.58 | 1.38 ▲ | 0.80 | 1 |
| A0A1X7VNC8 | Uncharacterized (RNA helicase family) | 1 | –0.04 | 1.47 ▲ | 1.51 | 3 |
| A0A1X7T7Q1 | Uncharacterized | 2 | –1.44 | –2.28 ▼ | –0.83 | 2 |

▲ and ▼ represent significant upregulation and downregulation, respectively. 'Proteins in cluster' indicate the number of identified proteins combined into each protein cluster.

Journal of Experimental Biology (2021) 224, jeb242820. doi:10.1242/jeb.242820

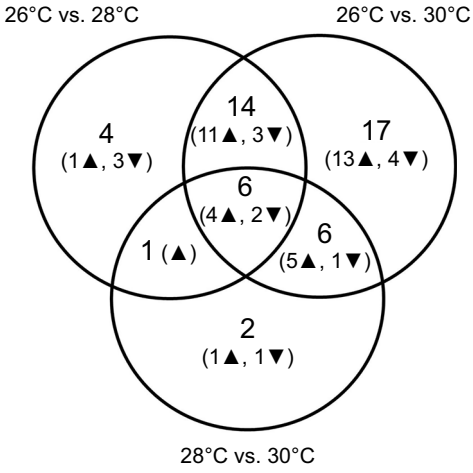


**Fig. 2. Venn diagram representing the distribution of the differentially abundant proteins from the marine sponge *A. navalis* exposed to different temperatures for 4 weeks.** Numbers in brackets represent the number of proteins that significantly increased (▲) or decreased (▼).

directly than is possible when using transcript-based gene expression analyses (Cox and Mann, 2007).

Proteomic analysis in the present study provided clear evidence of oxidative stress, which resulted in the increased abundance of multiple antioxidant enzymatic proteins, including aldehd-domain containing protein, catalase, thioredoxin-like superfamily and glutathione-S-transferase (Table 2). Increased abundance in these enzymatic proteins suggests an increase in detoxification processes to counteract the dissociation of amino acids by reactive oxygen species (ROS). ROS can be stimulated by heat stress in eukaryotes (Belhadj Slimen et al., 2014) and are often responsible for cellular damage (Ray et al., 2012). They have been reported in multiple marine organisms, such as corals (Lesser, 2006; Weis, 2008; Rosset et al., 2021) and the genetic upregulation of such enzymes as a response to oxidative stress has previously been reported in thermally stressed sponges (Bachinski et al., 1997; Pantile and Webster, 2011; Guzman and Conaco, 2016; González-Aravena et al., 2019). The increase in abundance of these enzymes in parallel with those of redox proteins, including ferritin and thioredoxin, suggests that *A. navalis* cells may be exposed to excess ROS at elevated temperature, requiring increased protein folding/refolding. The reduced abundance of cytochrome *c* proteins, which are known to dissociate in the presence of increased ROS concentrations in the cell, may also be indicative of an increase in cellular detoxification processes (Petrosillo et al., 2001; Min and Jian-xing, 2007). Consequently, it is likely that the increased oxygen consumption (i.e. increased metabolism) at higher temperature in *A. navalis* resulted in higher ROS generation.

Thermal stress also significantly increased the abundance of proteins related to cytoskeletal organization in *A. navalis*. The highest fold-changes in protein abundance were observed in costars-related protein, fascin and tubulin-α-related proteins (Table 2). These proteins are involved in cell motility (Pang et al., 2010) and the maintenance of cell shape, and provide mechanical resistance to cell deformation in the cytoskeleton complex (Herrmann et al., 2007). The increase in cytoskeletal activity observed here in *A. navalis* is most likely related to the loss of biomass (buoyant weight) of this sponge. The loss of biomass in sponges has often been attributed to environmental stress (Riisgård et al., 1993; Hadas et al., 2008). Under stress conditions, some sponges tend to reallocate their energetic resources used for growth and reproduction to sustain primary physiological functions such as respiration or pumping (Fang et al., 2014). The increased abundances of fascin and septin

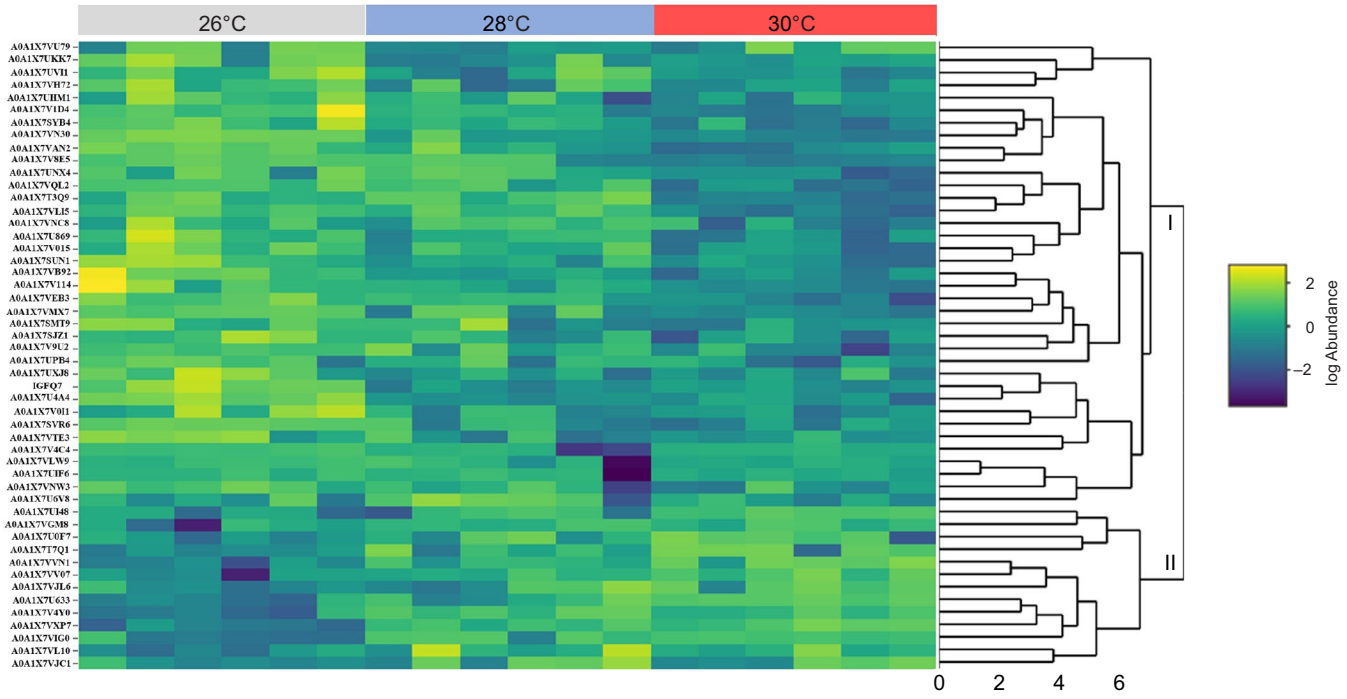


**Fig. 3. Heatmap showing the 50 differentially abundant proteins from the marine sponge *A. navalis* after a 4-week exposure to different temperatures.** Each row corresponds to a specific differentially abundant protein. Protein accession numbers are annotated in Table 2. Dendrogram demonstrates significant increase (I) and decrease (II) in protein abundance. Color scale ranges from yellow (low mean abundance) to dark blue (high mean abundance) and are relative to the mean abundance of all samples for each protein.

type-G, which are involved in functions such as cell migration (Yamashiro et al., 1998) and cell division (Bridges and Gladfelter, 2015), respectively, also demonstrate possible disruptions in cellular growth or organization of *A. navalis* cells. Tubulins are important components of the cytoskeleton complex and are involved in the formation and movement of cilia and flagella (Mohri et al., 2012). Given that sponges rely on the movement of flagellated cells for pumping and respiration, the increase in *A. navalis* pumping rate was likely associated with the increased abundances of multiple tubulin α-chain proteins (Green and Dove, 1984).

The enrichment of some proteins, such as proteasome subunit β (protein catabolism), ubiquitin (protein translation) and calmodulin (signal transduction), is consistent with previous thermal-stress studies performed on corals (Downs et al., 2000; DeSalvo et al., 2010; Huang et al., 2018). The enrichment of calmodulin, for example, has been reported in thermally stressed *Galexea astreata* (Huang et al., 2018). Increased presence of calmodulin suggests a possible disruption in $Ca^{2+}$ homeostasis, which could lead to disrupted cell proliferation (Berchtold and Villalobo, 2014). Being a multifunctional protein, calmodulin is involved in both signal transduction and cytoskeletal organization (Desrivières et al., 2002), and mediates multiple intracellular processes such as apoptosis and the immune response (Koga and Kawakami, 2018). As a result, the enrichment of proteins involved in intracellular proteolysis, protein tagging for degradation such as ubiquitin and proteasome subunit β, was not surprising. These proteins are more abundant during both cellular and physiological disorders (Schwartz and Ciechanover, 2009), and have been documented in thermally stressed corals such as *Orbicella faveolata* (Downs et al., 2000) and *Acropora palmata* (DeSalvo et al., 2010). The significant enrichment of proteasome subunit β and ubiquitin proteins in the present study suggests that *A. navalis* cells experienced increased protein folding stress at elevated temperature.

The proteomic responses of *A. navalis* reported here are partially consistent with the gene expression studies of Pantile and Webster (2011), Webster et al. (2013) and Guzman and Conaco (2016). However, it is interesting to note that the dynamics of some specific proteins reported for *A. navalis* differed from the gene expression of *R. odorabile* and *H. tubifera*. For example, while thermal stress reduced the expression of mRNA genes, such as calmodulin, ubiquitin and actin-related proteins, in *R. odorabile* (Pantile and Webster, 2011; Webster et al., 2013), these proteins were clearly more abundant in thermally stressed *A. navalis*. Furthermore, while both *R. odorabile* and *H. tubifera* experienced significant transcript upregulation of heat shock chaperones such as Hsp70 or Hsp90, no such enrichment was observed in the proteome of *A. navalis*. This variability in cellular biological functions may be attributed to the different temperature treatments (degree or duration) used in the different studies (Webster et al., 2013; Guzman and Conaco, 2016). For example, *R. odorabile* and *H. tubifera* were exposed to elevated temperatures for 3 days and 12 h, respectively, whereas in the present study, the thermal exposure of *A. navalis* was for 28 days. Heat shock responses often occur rapidly during the first few hours/days of thermal exposure (Tomanek, 2002). However, given the physiological–proteomic nature of this study, a short-term investigation (less than a week) would have prevented the acquisition of physiological data.

Protein abundance is a function of transcription rates, the availability of amino acids and ribosomes, protein degradation rates and other post-translational processes, and the mRNA–protein correlation can vary widely between genes (Cho, 2007; Buccitelli and Selbach, 2020). Therefore, the fundamental difference between transcript and protein measurements in cells experiencing thermal stress or other perturbations must be considered in experiments where cellular homeostasis is greatly impacted. Also, given that sponge physiological responses to elevated temperature are often species specific (Bell et al., 2018), this species specificity may also be reflected at the cellular level. The hypothesis that cellular responses in sponges might be species specific highlights the need to conduct additional in-depth multi-species proteomic investigations on the potential impacts of climate change on marine sponges. Furthermore, the high number of unidentified proteins reported in the present study (see Table S3), likely due to the phylogenetic distance between sponges and established model organisms, also highlights the need for better gene characterization in marine sponges.

Beepat et al. (2020) demonstrated that *A. navalis* was susceptible to elevated seawater temperature. Most sponges exposed to 30°C died after 10 days of experimental conditions. Surprisingly, no mortalities were recorded during the present study after the 4 weeks thermal exposure. This contrasting outcome is most likely due to the timing of the heat-stress experiments. While the former experiment was conducted near the end of winter (August to October), this study was carried out in peak summer conditions (December). According to McLachlan et al. (2020), the timing of heat-stress experiments can impact the outcomes of heat-stress investigations, because monthly maximum solar values differ significantly between summer and winter. As a result, the thermal maximum threshold in some organisms may sometimes be attenuated in summer seasons (Zhang et al., 2021). However, notwithstanding the contrasting timings of both experiments, the results of both studies clearly demonstrate that elevated temperature triggers thermal stress in the lagoon-inhabiting sponge *A. navalis*.

## Conclusions

Lagoon-inhabiting organisms are highly exposed to anthropogenic stressors. This study demonstrates that the lagoon-inhabiting sponge *A. navalis* will not tolerate thermal increases predicted under the RCP 6.0 and RCP 8.5 models (+2°C and +4°C, respectively). Sustained exposure to elevated seawater temperatures disrupted redox processes, protein transport and cytoskeletal organization of this sponge, leading to dysfunctional physiological performances. Consequently, this species may potentially disappear from its lagoonal habitats under future climate change scenarios. Our combined physiological–proteomic analysis shows that multidisciplinary approaches could greatly enhance our understanding of sponge stress and acclimation response mechanisms, and that such undertakings should be incorporated in future climate change and conservation management research.

#### Acknowledgements

We thank Akhilesh N. S. Beepat, Bhavna D. Ramlochun and Mohunlall Beepat for their assistance with fieldwork, laboratory setup and experimental procedures in Mauritius.

#### Competing interests

The authors declare no competing or financial interests.

#### Author contributions

Conceptualization: S.S.B., S.K.D., J.J.B.; Methodology: S.S.B., S.K.D., C.A.O., A.M., L.P., J.J.B.; Software: L.P.; Formal analysis: S.S.B.; Investigation: S.S.B.; Resources: S.K.D., C.A.O., A.M., L.P., J.J.B.; Writing - original draft: S.S.B.; Writing - review & editing: S.K.D., C.A.O., J.J.B.; Supervision: S.K.D., C.A.O., J.J.B.; Funding acquisition: S.S.B., S.K.D., C.A.O., J.J.B.

**Funding information**
This work was supported by the New Zealand Ministry of Foreign Affairs and Trade (4036 to S.S.B.). S.K.D. and C.A.O. were supported by the Royal Society of New Zealand Marsden Fund (VUW1601).

**Data availability**
Raw mass spectrometry data are available from the ProteomeXchange Consortium via the PRIDE partner repository with the dataset identifier: PXD027246.

**References**

**Achlatis, M., Van Der Zande, R. M., Schönberg, C. H. L., Fang, J. K. H., Hoegh-Guldberg, O. and Dove, S.** (2017). Sponge bioerosion on changing reefs: ocean warming poses physiological constraints to the success of a photosymbiotic excavating sponge. *Sci. Rep.* **7**, 10705. doi:10.1038/s41598-017-10947-1

**Anthony, A., Atwood, J., August, P., Byron, C., Cobb, S., Foster, C., Fry, C., Gold, A., Hagos, K., Heffner, L. et al.** (2009). Coastal lagoons and climate change: ecological and social ramifications in U.S. Atlantic and Gulf Coast ecosystems. *Ecol. Soc.* **14**, 8. doi:10.5751/ES-02719-140108

**Ávila, E. and Ortega-Bastida, A. L.** (2015). Influence of habitat and host morphology on macrofaunal assemblages associated with the sponge *Halichondria melanadocia* in an estuarine system of the southern Gulf of Mexico. *Mar. Ecol.* **36**, 1345-1353. doi:10.1111/maec.12233

**Bachinski, N., Koziol, C., Batel, R., Labura, Z., Schröder, H. C. and Müller, W. E. G.** (1997). Immediate early response of the marine sponge *Suberites domuncula* to heat stress: reduction of trehalose and glutathione concentrations and glutathione S-transferase activity. *J. Exp. Mar. Biol. Ecol.* **210**, 129-141. doi:10.1016/S0022-0981(96)02705-0

**Bates, T. E. M. and Bell, J. J.** (2018). Responses of two temperate sponge species to ocean acidification. *N. Z. J. Mar. Freshwat. Res.* **52**, 247-263. doi:10.1080/00288330.2017.1369132

**Beedessee, G., Ramanjooloo, A., Aubert, G., Eloy, L., Surnam-Boodhun, R., van Soest, R. W. M., Cresteil, T. and Marie, D. E. P.** (2012). Cytotoxic activities of hexane, ethyl acetate and butanol extracts of marine sponges from Mauritian Waters on human cancer cell lines. *Environ. Toxicol. Pharmacol.* **34**, 397-408. doi:10.1016/j.etap.2012.05.013

**Beepat, S. S.** (2015). *Ecology, Diversity and Symbiotic Associates (with special reference to Actinobacteria) of Marine Sponges in the Coastal Lagoons of Mauritius*. MPhil thesis, University of Mauritius, Reduit, Mauritius.

**Beepat, S. S., Appadoo, C., Marie, D. E., Paula, J. and Sivakumar, K.** (2013). Distribution, abundance and ecology of the sponge *Spheciospongia vagabunda* (phylum: Porifera, class: Demospongiae) in a shallow lagoon of Mauritius. *West. Indian Ocean J. Mar. Sci.* **12**, 15-23.

**Beepat, S. S., Appadoo, C., Marie, D. E. P., Paula, J., Çinar, M. and Sivakumar, K.** (2014). Macrofauna associated with the sponge *Neopetrosia exigua* (Kirkpatrick, 1900) in Mauritius. *West. Indian Ocean J. Mar. Sci.* **13**, 133-142.

**Beepat, S. S., Davy, S. K., Woods, L. and Bell, J. J.** (2020). Short-term responses of tropical lagoon sponges to elevated temperature and nitrate. *Mar. Environ. Res.* **157**, 104922. doi:10.1016/j.marenvres.2020.104922

**Belhadj Slimen, I., Najar, T., Ghram, A., Dabbebi, H., Ben Mrad, M. and Abdrabbah, M.** (2014). Reactive oxygen species, heat stress and oxidative-induced mitochondrial damage. A review. *Int. J. Hyperth.* **30**, 513-523. doi:10.3109/02656736.2014.971446

**Bell, J. J.** (2008). The functional roles of marine sponges. *Estuar. Coast. Shelf Sci.* **79**, 341-353. doi:10.1016/j.ecss.2008.05.002

**Bell, J. J., Bennett, H. M., Rovellini, A. and Webster, N. S.** (2018). Sponges to be winners under near-future climate scenarios. *Bioscience* **68**, 955-968. doi:10.1093/biosci/biy142

**Bennett, H. M., Altenrath, C., Woods, L., Davy, S. K., Webster, N. S. and Bell, J. J.** (2017). Interactive effects of temperature and $pCO_2$ on sponges: from the cradle to the grave. *Global Change Biol.* **23**, 2031-2046. doi:10.1111/gcb.13474

**Berchtold, M. W. and Villalobo, A.** (2014). The many faces of calmodulin in cell proliferation, programmed cell death, autophagy, and cancer. *Biochim. Biophys. Acta Mol. Cell Res.* **1843**, 398-435. doi:10.1016/j.bbamcr.2013.10.021

**Biggerstaff, A., Smith, D. J., Jompa, J. and Bell, J. J.** (2015). Photoacclimation supports environmental tolerance of a sponge to turbid low-light conditions. *Coral Reefs* **34**, 1049-1061. doi:10.1007/s00338-015-1340-9

**Binns, D., Dimmer, E., Huntley, R., Barrell, D., O'donovan, C. and Apweiler, R.** (2009). QuickGO: a web-based tool for gene ontology searching. *Bioinformatics* **25**, 3045-3046. doi:10.1093/bioinformatics/btp536

**Bridges, A. A. and Gladfelter, A. S.** (2015). Septin form and function at the cell cortex. *J. Biol. Chem.* **290**, 17173-17180. doi:10.1074/jbc.R114.634444

**Buccitelli, C. and Selbach, M.** (2020). mRNAs, proteins and the emerging principles of gene expression control. *Nat. Rev. Genet.* **21**, 630-644. doi:10.1038/s41576-020-0258-4

**Cerrano, C., Pansini, M., Valisano, L., Calcinai, B., Sarà, M. and Bavestrello, G.** (2004). Lagoon sponges from Carrie Bow Cay (Belize): ecological benefits of selective sediment incorporation. *Bollettino dei Musei e degli Istituti Biologici dell'Univesita di Genova* 68, 239-252.

**Chaib De Mares, M., Jiménez, D. J., Palladino, G., Gutleben, J., Lebrun, L. A., Muller, E. E. L., Wilmes, P., Sipkema, D. and Van Elsas, J. D.** (2018). Expressed protein profile of a Tectomicrobium and other microbial symbionts in the marine sponge *Aplysina aerophoba* as evidenced by metaproteomics. *Sci. Rep.* **8**, 11795. doi:10.1038/s41598-018-30134-0

**Cho, W. C. S.** (2007). Proteomics technologies and challenges. *Genomics Proteomics Bioinform.* **5**, 77-85. doi:10.1016/S1672-0229(07)60018-7

**Cox, J., Hein, M. Y., Luber, C. A., Paron, I., Nagaraj, N. and Mann, M.** (2014). Accurate proteome-wide label-free quantification by delayed normalization and maximal peptide ratio extraction, termed MaxLFQ. *Mol. Cell. Proteomics* **13**, 2513-2526. doi:10.1074/mcp.M113.031591

**Cox, J. and Mann, M.** (2007). Is proteomics the new genomics? *Cell* **130**, 395-398. doi:10.1016/j.cell.2007.07.032

**De Goeij, J. M., Van Oevelen, D., Vermeij, M. J. A., Osinga, R., Middelburg, J. J., De Goeij, A. F. P. M. and Admiraal, W.** (2013). Surviving in a marine desert: The sponge loop retains resources within coral reefs. *Science* **342**, 108-110. doi:10.1126/science.1241981

**De Goeij, J. M., Lesser, M. P. and Pawlik, J. R.** (2017). Nutrient fluxes and ecological functions of coral reef sponges in a changing ocean. In *Climate Change, Ocean Acidification and Sponges* (ed. J. L. Carballo and J. J. Bell), pp. 373-410. Cham: Springer International Publishing.

**Desalvo, M. K., Sunagawa, S., Voolstra, C. R. and Medina, M.** (2010). Transcriptomic responses to heat stress and bleaching in the elkhorn coral *Acropora palmata*. *Mar. Ecol. Prog. Ser.* **402**, 97-113. doi:10.3354/meps08372

**Desrivières, S., Cooke, F. T., Morales-Johansson, H., Parker, P. J. and Hall, M. N.** (2002). Calmodulin controls organization of the actin cytoskeleton *via* regulation of phosphatidylinositol (4,5)-bisphosphate synthesis in *Saccharomyces cerevisiae*. *Biochem. J.* **366**, 945-951. doi:10.1042/bj20020429

**Downs, C. A., Mueller, E., Phillips, S., Fauth, J. E. and Woodley, C. M.** (2000). A molecular biomarker system for assessing the health of coral (*Montastraea faveolata*) during heat stress. *Mar. Biotechnol.* **2**, 533-544. doi:10.1007/s101260000038

**Duckworth, A. R. and Peterson, B. J.** (2013). Effects of seawater temperature and pH on the boring rates of the sponge *Cliona celata* in scallop shells. *Mar. Biol.* **160**, 27-35. doi:10.1007/s00227-012-2053-z

**Duckworth, A. R., West, L., Vansach, T., Stubler, A. and Hardt, M.** (2012). Effects of water temperature and pH on growth and metabolite biosynthesis of coral reef sponges. *Mar. Ecol. Prog. Ser.* **462**, 67-77. doi:10.3354/meps09853

**Eden, E., Geva-Zatorsky, N., Issaeva, I., Cohen, A., Dekel, E., Danon, T., Cohen, L., Mayo, A. and Alon, U.** (2011). Proteome half-life dynamics in living human cells. *Science* **331**, 764-768. doi:10.1126/science.1199784

**Fagoonee, I.** (1990). Coastal marine ecosystems of Mauritius. *Hydrobiologia* **208**, 55-62. doi:10.1007/BF00008443

**Fan, L., Liu, M., Simister, R., Webster, N. S. and Thomas, T.** (2013). Marine microbial symbiosis heats up: the phylogenetic and functional response of a sponge holobiont to thermal stress. *ISME J.* **7**, 991-1002. doi:10.1038/ismej.2012.165

**Fang, J. K. H., Schönberg, C. H. L., Mello-Athayde, M. A., Hoegh-Guldberg, O. and Dove, S.** (2014). Effects of ocean warming and acidification on the energy budget of an excavating sponge. *Global Change Biol.* **20**, 1043-1054. doi:10.1111/gcb.12369

**González-Aravena, M., Kenny, N. J., Osorio, M., Font, A., Riesgo, A. and Cárdenas, C. A.** (2019). Warm temperatures, cool sponges: the effect of increased temperatures on the Antarctic sponge *Isodictya* sp. *PeerJ* **7**, e8088. doi:10.7717/peerj.8088

**Green, L. L. and Dove, W. F.** (1984). Tubulin proteins and RNA during the myxamoeba-flagellate transformation of *Physarum polycephalum*. *Mol. Cell. Biol.* **4**, 1706-1711.

**Guzman, C. and Conaco, C.** (2016). Gene expression dynamics accompanying the sponge thermal stress response. *PLoS ONE* **11**, e0165368. doi:10.1371/journal.pone.0165368

**Hadas, E., Ilan, M. and Shpigel, M.** (2008). Oxygen consumption by a coral reef sponge. *J. Exp. Biol.* **211**, 2185-2190. doi:10.1242/jeb.015420

**Herrmann, H., Bär, H., Kreplak, L., Strelkov, S. V. and Aebi, U.** (2007). Intermediate filaments: from cell architecture to nanomechanics. *Nat. Rev. Mol. Cell Biol.* **8**, 562-573. doi:10.1038/nrm2197

**Hoegh-Guldberg, O.** (1999). Climate change, coral bleaching and the future of the world's coral reefs. *Mar. Freshwat. Res.* **50**, 839-866. doi:10.1071/MF99078

**Huang, Y., Yuan, J., Zhang, Y., Peng, H. and Liu, L.** (2018). Molecular cloning and characterization of calmodulin-like protein CaLP from the scleractinian coral *Galaxea astreata*. *Cell Stress Chaperones* **23**, 1329-1335. doi:10.1007/s12192-018-0907-0

**Ilan, M. and Abelson, A.** (1995). The life of a sponge in a sandy lagoon. *Biol. Bull.* **189**, 363-369. doi:10.2307/1542154

**IPCC** (2014). Climate change (2014): synthesis report. In *Contribution of working groups I, II and III to the Fifth Assessment Report of the Intergovernmental Panel on Climate Change* (ed. R. K. Pachauri and L. A. Meyer), pp. 75-91. Geneva, Switzerland: IPCC.

**Kennish, M. J.** (2016). Coastal Lagoons. In *Encyclopedia of Estuaries* (ed. M. J. Kennish), pp. 29-35. Dordrecht: Springer Netherlands.
**Kennish, M. J. and Paerl, H. W.** (2010). *Coastal Lagoons: Critical Habitats of Environmental Change*, CRC Press.
**Koga, T. and Kawakami, A.** (2018). The role of CaMK4 in immune responses. *Mod. Rheumatol.* **28**, 211-214. doi:10.1080/14397595.2017.1413964
**Koutsouveli, V., Manousaki, T., Riesgo, A., Lagnel, J., Kollias, S., Tsigenopoulos, C. S., Arvanitidis, C., Dounas, C., Magoulas, A. and Dailianis, T.** (2020). Gearing up for warmer times: transcriptomic response of *Spongia officinalis* to elevated temperatures reveals recruited mechanisms and potential for resilience. *Front. Mar. Sci.* **6**, 786. doi:10.3389/fmars.2019.00786
**Krasko, A., Scheffer, U., Koziol, C., Pancer, Z., Batel, R., Badria, F. A. and Müller, W. E. G.** (1997). Diagnosis of sublethal stress in the marine sponge *Geodia cydonium*: application of the 70 kDa heat-shock protein and a novel biomarker, the Rab GDP dissociation inhibitor, as probes. *Aquat. Toxicol.* **37**, 157-168. doi:10.1016/S0166-445X(96)00822-3
**Lesser, M. P.** (2006). Oxidative stress in marine environments: biochemistry and physiological ecology. *Annu. Rev. Physiol.* **68**, 253-278. doi:10.1146/annurev.physiol.68.040104.110001
**Levi, C., Laboute, P., Bargibant, G. and Menou, J.** (1998). *Sponges from the New Caledonian Lagoon*. Paris, France: Orstom.
**Leys, S. P., Yahel, G., Reidenbach, M. A., Tunnicliffe, V., Shavit, U. and Reiswig, H. M.** (2011). The sponge pump: the role of current induced flow in the design of the sponge body plan. *PLoS ONE* **6**, e27787. doi:10.1371/journal.pone.0027787
**Liu, M., Fan, L., Zhong, L., Kjelleberg, S. and Thomas, T.** (2012). Metaproteogenomic analysis of a community of sponge symbionts. *ISME J.* **6**, 1515-1525. doi:10.1038/ismej.2012.1
**López-Legentil, S., Song, B., Mcmurray, S. E. and Pawlik, J. R.** (2008). Bleaching and stress in coral reef ecosystems: hsp70 expression by the giant barrel sponge *Xestospongia muta*. *Mol. Ecol.* **17**, 1840-1849. doi:10.1111/j.1365-294X.2008.03667.x
**Maldonado, M., Ribes, M. and Van Duyl, F. C.** (2012). Nutrient fluxes through sponges: biology, budgets, and ecological implications. *Adv. Mar. Biol.* **62**, 113-182. doi:10.1016/B978-0-12-394283-8.00003-5
**Massaro, A. J., Weisz, J. B., Hill, M. S. and Webster, N. S.** (2012). Behavioral and morphological changes caused by thermal stress in the great barrier reef sponge *Rhopaloeides odorabile*. *J. Exp. Mar. Biol. Ecol.* **416-417**, 55-60. doi:10.1016/j.jembe.2012.02.008
**Mcclanahan, T. R., Ateweberhan, M., Muhando, C. A., Maina, J. and Mohammed, M. S.** (2007). Effects of climate and seawater temperature variation on coral bleaching and mortality. *Ecol. Monogr.* **77**, 503-525. doi:10.1890/06-1182.1
**Mcclanahan, T. R., Maina, J. M. and Muthiga, N. A.** (2011). Associations between climate stress and coral reef diversity in the western Indian Ocean. *Global Change Biol.* **17**, 2023-2032. doi:10.1111/j.1365-2486.2011.02395.x
**McLachlan, R. H., Price, J. T., Solomon, S. L. and Grottoli, A. G.** (2020). Thirty years of coral heat-stress experiments: a review of methods. *Coral Reefs* **39**, 885-902. doi:10.1007/s00338-020-01931-9
**Miller, A., Strychar, K., Shirley, T. and Rützler, K.** (2010). Effects of heat and salinity stress on the sponge *Cliona Celata*. *Int. J. Biol.* **2**, 3-16. doi:10.5539/ijb.v2n2p3
**Min, L. and Jian-Xing, X.** (2007). Detoxifying function of cytochrome c against oxygen toxicity. *Mitochondrion* **7**, 13-16. doi:10.1016/j.mito.2006.11.011
**Mohri, H., Inaba, K., Ishijima, S. and Baba, S. A.** (2012). Tubulin-dynein system in flagellar and ciliary movement. *Proc. Jpn Acad. Ser. B Phys. Biol. Sci.* **88**, 397-415. doi:10.2183/pjab.88.397
**Oakley, C. A., Ameismeier, M. F., Peng, L., Weis, V. M., Grossman, A. R. and Davy, S. K.** (2016). Symbiosis induces widespread changes in the proteome of the model cnidarian *Aiptasia*. *Cell. Microbiol.* **18**, 1009-1023. doi:10.1111/cmi.12564
**Oakley, C. A., Durand, E., Wilkinson, S. P., Peng, L., Weis, V. M., Grossman, A. R. and Davy, S. K.** (2017). Thermal shock induces host proteostasis disruption and endoplasmic reticulum stress in the model symbiotic Cnidarian Aiptasia. *J. Proteome Res.* **16**, 2121-2134. doi:10.1021/acs.jproteome.6b00797
**Osinga, R., Redeker, D., Beukelaar, P. B. and Wijffels, R.** (1999). Measurement of sponge growth by projected body area and underwater weight. *Mem. Queensland Meusem* **44**, 419-426.
**Pang, T.-L., Chen, F.-C., Weng, Y.-L., Liao, H.-C., Yi, Y.-H., Ho, C.-L., Lin, C.-H. and Chen, M.-Y.** (2010). Costars, a *Dictyostelium* protein similar to the C-terminal domain of STARS, regulates the actin cytoskeleton and motility. *J. Cell Sci.* **123**, 3745-3755. doi:10.1242/jcs.064709
**Pantile, R. and Webster, N.** (2011). Strict thermal threshold identified by quantitative PCR in the sponge *Rhopaloeides odorabile*. *Mar. Ecol. Prog. Ser.* **431**, 97-105. doi:10.3354/meps09128
**Perez-Riverol, Y., Csordas, A., Bai, J., Bernal-Llinares, M., Hewapathirana, S., Kundu, D. J., Inuganti, A., Griss, J., Mayer, G., Eisenacher, M. et al.** (2019). The PRIDE database and related tools and resources in 2019: improving support for quantification data. *Nucleic Acids Res.* **47**, D442-D450. doi:10.1093/nar/gky1106
**Pérez-Ruzafa, A., Pérez-Ruzafa, I. M., Newton, A. and Marcos, C.** (2019). Coastal lagoons: environmental variability, ecosystem complexity, and goods and services uniformity. In *Coasts and Estuaries* (ed. E. Wolanski, J. W. Day, M. Elliott and R. Ramachandran), pp. 253-276. Elsevier. doi:10.1016/B978-0-12-814003-1.00015-0
**Petrosillo, G., Ruggiero, F. M., Pistolese, M. and Paradies, G.** (2001). Reactive oxygen species generated from the mitochondrial electron transport chain induce cytochrome c dissociation from beef-heart submitochondrial particles via cardiolipin peroxidation. Possible role in the apoptosis. *FEBS Lett.* **509**, 435-438. doi:10.1016/S0014-5793(01)03206-9
**Pulitzer-Finali, G.** (1993). A collection of marine sponges from East Africa. *Annali del Museo Civico di Storia Naturale Giacomo Doria* 89, 247-350.
**Ray, P. D., Huang, B.-W. and Tsuji, Y.** (2012). Reactive oxygen species (ROS) homeostasis and redox regulation in cellular signaling. *Cell. Signal.* **24**, 981-990. doi:10.1016/j.cellsig.2012.01.008
**Reiswig, H. M.** (1971). In situ pumping activities of tropical Demospongiae. *Mar. Biol.* **9**, 38-50. doi:10.1007/BF00348816
**Riisgård, H. U., Thomassen, S., Jakobsen, H., Weeks, J. M. and Larsen, P. S.** (1993). Suspension feeding in marine sponges *Halichondria panicea* and *Haliclona urceolus*: effects of temperature on filtration rate and energy cost of pumping. *Mar. Ecol. Prog. Ser.* **96**, 177-188. doi:10.3354/meps096177
**Rix, L., de Goeij, J. M., van Oevelen, D., Struck, U., Al-Horani, F. A., Wild, C. and Naumann, M. S.** (2018). Reef sponges facilitate the transfer of coral-derived organic matter to their associated fauna via the sponge loop. *Mar. Ecol. Prog. Ser.* **589**, 85-96. doi:10.3354/meps12443
**Rosset, S. L., Oakley, C. A., Ferrier-Pagès, C., Suggett, D. J., Weis, V. M. and Davy, S. K.** (2021). The molecular language of the Cnidarian–Dinoflagellate Symbiosis. *Trends Microbiol.* **29**, 320-333. doi:10.1016/j.tim.2020.08.005
**Schwämmle, V., Hagensen, C. E., Rogowska-Wrzesinska, A. and Jensen, O. N.** (2020). PolySTest: robust statistical testing of proteomics data with missing values improves detection of biologically relevant features. *Mol. Cell. Proteomics* **19**, 1396-1408. doi:10.1074/mcp.RA119.001777
**Schwartz, A. L. and Ciechanover, A.** (2009). Targeting proteins for destruction by the ubiquitin system: implications for human pathobiology. *Annu. Rev. Pharmacol. Toxicol.* **49**, 73-96. doi:10.1146/annurev.pharmtox.051208.165340
**Sproles, A. E., Oakley, C. A., Matthews, J. L., Peng, L., Owen, J. G., Grossman, A. R., Weis, V. M. and Davy, S. K.** (2019). Proteomics quantifies protein expression changes in a model cnidarian colonised by a thermally tolerant but suboptimal symbiont. *ISME J.* **13**, 2334-2345. doi:10.1038/s41396-019-0437-5
**Srivastava, M., Simakov, O., Chapman, J., Fahey, B., Gauthier, M. E. A., Mitros, T., Richards, G. S., Conaco, C., Dacre, M., Hellsten, U. et al.** (2010). The *Amphimedon queenslandica* genome and the evolution of animal complexity. *Nature* **466**, 720-726. doi:10.1038/nature09201
**Tisthammer, K. H., Timmins-Schiffman, E., Seneca, F. O., Nunn, B. L. and Richmond, R. H.** (2021). Physiological and molecular responses of lobe coral indicate nearshore adaptations to anthropogenic stressors. *Sci. Rep.* **11**, 3423. doi:10.1038/s41598-021-82569-7
**Tomanek, L.** (2002). The heat-shock response: its variation, regulation and ecological importance in intertidal gastropods (genus *Tegula*). *Integr. Comp. Biol.* **42**, 797-807. doi:10.1093/icb/42.4.797
**Turner, J., Hardman, E., Klaus, R., Fagoonee, I., Daby, D., Baghooli, R. and Persands, S.** (2000). *The reefs of*
**Tyanova, S. and Cox, J.** (2018). Perseus: A bioinformatics platform for integrative analysis of proteomics data in cancer research. In *Cancer Systems Biology: Methods and Protocols* (ed. L. Von Stechow), pp. 133-148. New York: Springer.
**Tyers, M. and Mann, M.** (2003). From genomics to proteomics. *Nature* **422**, 193-197. doi:10.1038/nature01510
**Vogel, C. and Marcotte, E. M.** (2012). Insights into the regulation of protein abundance from proteomic and transcriptomic analyses. *Nat. Rev. Genet.* **13**, 227-232. doi:10.1038/nrg3185
**Webster, N., Pantile, R., Botté, E., Abdo, D., Andreakis, N. and Whalan, S.** (2013). A complex life cycle in a warming planet: gene expression in thermally stressed sponges. *Mol. Ecol.* **22**, 1854-1868. doi:10.1111/mec.12213
**Weis, V. M.** (2008). Cellular mechanisms of Cnidarian bleaching: stress causes the collapse of symbiosis. *J. Exp. Biol.* **211**, 3059-3066. doi:10.1242/jeb.009597
**Wiśniewski, J. R., Zougman, A., Nagaraj, N. and Mann, M.** (2009). Universal sample preparation method for proteome analysis. *Nat. Methods* **6**, 359-362. doi:10.1038/nmeth.1322
**Wulff, J. L.** (2006). Ecological interactions of marine sponges. *Can. J. Zool.* **84**, 146-166. doi:10.1139/z06-019
**Wulff, J. L.** (2016). Sponge contributions to the geology and biology of reefs: past, present, and future. In *Coral Reefs at the Crossroads* (ed. D. K. Hubbard, C. S. Rogers, J. H. Lipps and J. G. D. Stanley), pp. 103-126. Dordrecht: Springer Netherlands.
**Yamashiro, S., Yamakita, Y., Ono, S. and Matsumura, F.** (1998). Fascin, an actin-bundling protein, induces membrane protrusions and increases cell motility of epithelial cells. *Mol. Biol. Cell* **9**, 993-1006. doi:10.1091/mbc.9.5.993

**Yeung, Y.-G. and Stanley, E. R.** (2010). Chapter 16. Rapid detergent removal from peptide samples with ethyl acetate for mass spectrometry analysis. In *Curr. Protoc. Protein Sci.* 59, 16.12.1-16.12.5. doi:10.1002/0471140864.ps1612s59

**Zhang, W.-y., Story, K. B. and Dong, Y.-w.** (2021). Synchronization of seasonal acclimatization and short-term heat hardening improves physiological resilience in a changing climate. *Funct. Ecol.* **35**, 686-695. doi:10.1111/1365-2435.13768

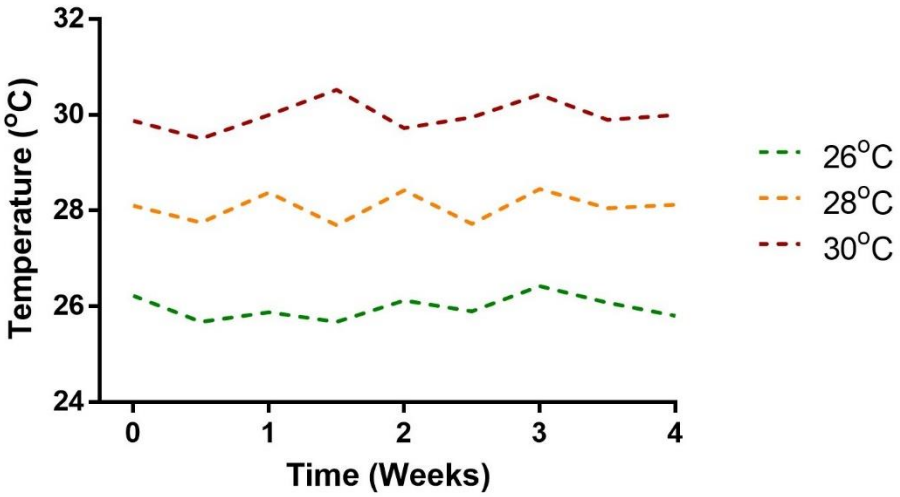


**Fig. S1.** Temperature fluctuations in treatment tanks during the experiments. Reported values were measured daily at 3-hours intervals using temperature loggers.

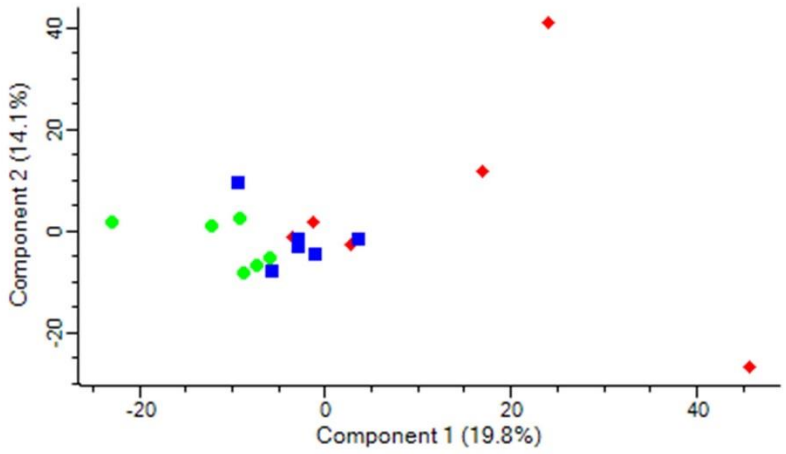


**Fig. S2.** Principal Component Analysis (PCA) plot of significantly abundant proteins in *Amphimedon navalis* at 26 ºC (filled circles), 28 ºC (filled squares) and 30 ºC (filled diamonds). PCA was constructed using all detected proteins. Each point represents a biological sponge replicate (n = 6 *per* treatment).

**Table S1.** Results of time * temperature *post hoc* pairwise comparisons test (with the sequential Sidak correction applied) from general linear mixed models for percentage change in buoyant weight, holobiont oxygen consumption and pumping rates of *Amphimedon navalis* in response to elevated temperature. Significant p-values are reported in bold. (n = 9 *per* treatment *per* time point)

| Time (Weeks) | Temp | | Contrast Estimate | Std. Error | t | df | *P* | CI (lower) | CI (upper) |
|---|---|---|---|---|---|---|---|---|---|
| **Buoyant weight** | | | | | | | | | |
| **0** | 28ºC | 26ºC | - | - | - | - | - | - | - |
| | 30ºC | 26ºC | - | - | - | - | - | - | - |
| | 30ºC | 28ºC | - | - | - | - | - | - | - |
| **1** | 28ºC | 26ºC | -0.007 | 0.002 | -2.830 | 60 | **0.013** | -0.013 | -0.001 |
| | 30ºC | 26ºC | -0.009 | 0.002 | -3.620 | 60 | **0.002** | -0.015 | -0.003 |
| | 30ºC | 28ºC | -0.002 | 0.002 | -0.790 | 60 | 0.433 | -0.007 | 0.003 |
| **2** | 28ºC | 26ºC | -0.012 | 0.002 | -4.783 | 60 | **<0.001** | -0.017 | -0.006 |
| | 30ºC | 26ºC | -0.018 | 0.002 | -7.280 | 60 | **<0.001** | -0.024 | -0.012 |
| | 30ºC | 28ºC | -0.006 | 0.002 | -2.497 | 60 | **0.015** | -0.011 | -0.001 |
| **3** | 28ºC | 26ºC | -0.016 | 0.002 | -6.537 | 60 | **<0.001** | -0.022 | -0.010 |
| | 30ºC | 26ºC | -0.026 | 0.002 | -10.396 | 60 | **<0.001** | -0.032 | -0.020 |
| | 30ºC | 28ºC | -0.010 | 0.002 | -3.859 | 60 | **<0.001** | -0.014 | -0.005 |
| **4** | 28ºC | 26ºC | -0.020 | 0.002 | -8.209 | 60 | **<0.001** | -0.026 | -0.015 |
| | 30ºC | 26ºC | -0.034 | 0.002 | -13.751 | 60 | **<0.001** | -0.040 | -0.028 |
| | 30ºC | 28ºC | -0.014 | 0.002 | -5.542 | 60 | **<0.001** | -0.019 | -0.009 |
| ***Holobiont oxygen consumption rate*** | | | | | | | | | |
| **0** | 28ºC | 26ºC | -0.001 | 0.003 | -0.247 | 27 | 0.993 | -0.009 | 0.007 |
| | 30ºC | 26ºC | -0.001 | 0.003 | -0.003 | 27 | 0.998 | -0.007 | 0.006 |
| | 30ºC | 28ºC | 0.001 | 0.003 | 0.245 | 27 | 0.993 | -0.007 | 0.009 |
| **1** | 28ºC | 26ºC | 0.003 | 0.003 | 1.066 | 27 | 0.504 | -0.004 | 0.011 |
| | 30ºC | 26ºC | 0.005 | 0.003 | 1.687 | 27 | 0.279 | -0.003 | 0.013 |
| | 30ºC | 28ºC | 0.002 | 0.003 | 0.621 | 27 | 0.540 | -0.005 | 0.008 |
| **2** | 28ºC | 26ºC | 0.005 | 0.003 | 1.539 | 27 | 0.135 | -0.002 | -0.004 |
| | 30ºC | 26ºC | 0.012 | 0.003 | 3.670 | 27 | **0.003** | 0.004 | 0.020 |
| | 30ºC | 28ºC | 0.007 | 0.003 | 2.131 | 27 | 0.083 | -0.001 | 0.014 |
| **3** | 28ºC | 26ºC | 0.007 | 0.003 | 2.224 | 27 | **0.035** | 0.001 | 0.014 |
| | 30ºC | 26ºC | 0.016 | 0.003 | 5.159 | 27 | **<0.001** | 0.008 | 0.024 |
| | 30ºC | 28ºC | 0.009 | 0.003 | 2.935 | 27 | **0.014** | 0.002 | 0.017 |
| **4** | 28ºC | 26ºC | 0.009 | 0.003 | 2.690 | 27 | **0.012** | 0.002 | 0.015 |
| | 30ºC | 26ºC | 0.020 | 0.003 | 6.224 | 27 | **<0.001** | 0.012 | 0.028 |
| | 30ºC | 28ºC | 0.011 | 0.003 | 3.534 | 27 | **0.003** | 0.004 | 0.019 |

| Time (Weeks) | Temp | | Contrast Estimate | Std. Error | t | df | *P* | CI (lower) | CI (upper) |
|---|---|---|---|---|---|---|---|---|---|
| | | | | ***Pumping rate*** | | | | | |
| | 28ºC | 26ºC | 0.008 | 0.003 | 2.801 | 38 | **0.024** | 0.001 | 0.015 |
| **0** | 30ºC | 26ºC | 0.006 | 0.003 | 2.032 | 38 | 0.096 | -0.001 | 0.013 |
| | 30ºC | 28ºC | -0.002 | 0.003 | -0.769 | 38 | 0.447 | -0.008 | 0.004 |
| | 28ºC | 26ºC | 0.009 | 0.003 | 3.273 | 38 | **0.005** | 0.003 | 0.016 |
| **1** | 30ºC | 26ºC | 0.013 | 0.003 | 4.404 | 38 | **<0.001** | 0.005 | 0.020 |
| | 30ºC | 28ºC | 0.003 | 0.003 | 1.131 | 38 | 0.265 | -0.003 | 0.009 |
| | 28ºC | 26ºC | 0.010 | 0.003 | 3.338 | 38 | **0.004** | 0.003 | 0.016 |
| **2** | 30ºC | 26ºC | 0.018 | 0.003 | 6.431 | 38 | **<0.001** | 0.011 | 0.026 |
| | 30ºC | 28ºC | 0.009 | 0.003 | 3.094 | 38 | **0.004** | 0.003 | 0.015 |
| | 28ºC | 26ºC | 0.020 | 0.003 | 6.999 | 38 | **<0.001** | 0.013 | 0.027 |
| **3** | 30ºC | 26ºC | 0.033 | 0.003 | 11.401 | 38 | **<0.001** | 0.026 | 0.040 |
| | 30ºC | 28ºC | 0.013 | 0.003 | 4.402 | 38 | **<0.001** | 0.007 | 0.018 |
| | 28ºC | 26ºC | 0.022 | 0.003 | 7.743 | 38 | **<0.001** | 0.016 | 0.029 |
| **4** | 30ºC | 26ºC | 0.040 | 0.003 | 13.980 | 38 | **<0.001** | 0.003 | 0.047 |
| | 30ºC | 28ºC | 0.018 | 0.003 | 6.237 | 38 | **<0.001** | 0.012 | 0.024 |

**Table S2.** Results of pairwise comparisons between temperature treatments for differentially abundant proteins from *Amphimedon navalis* from Miss test using an FDR threshold of 0.1 and log-ratio (fold-change) of ±0.25. Significant p-values are reported in bold.

| Uniprot Accession number | Protein annotation | Proteins in cluster | 26ºC vs 28ºC | 26ºC vs 30ºC | 28ºC vs 30ºC |
|---|---|---|---|---|---|
| **Oxidation-reduction process (Oxidative stress)** | | | | | |
| A0A1X7V4C4 | Aldedh domain-containing protein | 2 | **1.22E-05** | **5.24E-06** | 0.980313 |
| I1GFQ7 | Ferritin | 2 | **3.53E-06** | **5.24E-06** | 1 |
| A0A1X7SUN1 | VOC domain-containing protein | 2 | 0.831446 | **0.054828** | 1 |
| A0A1X7VNW3 | Catalase (Heme cofactor) | 2 | 0.311372 | **0.001572** | **0.090423** |
| A0A1X7VQL2 | Uncharacterized (Thioredoxin-like superfamily) | 1 | 1 | **0.012566** | **0.090423** |
| A0A1X7UNX4 | Uncharacterized (Glutathione S-transferase superfamily) | 1 | 1 | 0.192653 | **0.050264** |
| A0A1X7T3Q9 | E1_dh domain-containing protein | 2 | 1 | **0.000314** | **0.003458** |
| A0A1X7VJL6 | Peroxiredoxin | 1 | 0.83146 | **0.049142** | **1** |
| A0A1X7U633 | Cytochrome c domain-containing protein | 2 | 0.795518 | **0.000314** | **0.035267** |
| A0A1X7V4Y0 | Proton-translocating NAD(P) (+) transhydrogenase | 1 | **0.071665** | **0.063899** | 0.683634 |
| **Protein transport** | | | | | |
| A0A1X7U4A4 | Protein kinase domain-containing protein | 1 | **0.023796** | **0.047885** | 1 |
| A0A1X7UVI1 | Protein kinase domain-containing protein | 1 | 0.559622 | **0.042849** | 0.683634 |
| A0A1X7VH72 | Uncharacterized (inositol phosphokinase family) | 1 | **0.066834** | **0.012566** | 1 |
| A0A1X7V114 | Vacuolar protein sorting-associated protein 11 homolog | 1 | 0.63163 | **0.001937** | 0.115427 |
| A0A1X7UHM1 | Ras-related protein Rab-14 | 1 | 1 | **0.055495** | 0.40943 |
| A0A1X7VLI5 | Protein kinase domain-containing protein | 1 | 1 | **0.005623** | **0.03029** |
| A0A1X7VL10 | ATP synthase subunit beta | 1 | **0.023366** | 0.207581 | 1 |
| A0A1X7VVN1 | Uncharacterized (ABC transporter-like family) | 1 | **0.066834** | **0.001133** | **0.079628** |
| A0A1X7VJC1 | Uncharacterized (DUOXA family) | 1 | **0.024449** | 0.222406 | 0.683634 |
| A0A1X7VXP7 | Uncharacterized (SNF7 family) | 1 | **0.015008** | **0.003536** | 0.61806 |
| **Cytoskeletal organization** | | | | | |
| A0A1X7UKK7 | Costars domain-containing protein | 1 | **0.066834** | **0.001937** | 0.61806 |
| A0A1X7VU79 | Fascin | 1 | **0.066834** | 0.2606 | 0.40943 |
| A0A1X7UPB4 | Tubulin alpha chain | 1 | **0.066834** | **0.000171** | 0.393734 |
| A0A1X7UIF6 | F-actin-capping protein subunit beta | 1 | 1 | 0.680671 | **0.079628** |
| A0A1X7V1D4 | Tubulin alpha chain | 1 | **0.024449** | **5.24E-06** | **0.005016** |
| A0A1X7U6V8 | Septin-type G domain-containing protein | 2 | **0.047777** | 1 | **0.005016** |
| A0A1X7VTE3 | Uncharacterized (small GTPase family) | 1 | 0.232523 | **0.005506** | 0.269237 |
| A0A1X7UXJ8 | Uncharacterized (alpha-actinin family) | 1 | **0.023366** | **0.008162** | **1** |
| A0A1X7V9U2 | Uncharacterized (WASH complex, subunit strumpellin) | 1 | 1 | **0.033781** | **0.090423** |
| A0A1X7U0F7 | PDZ domain-containing protein | 1 | 1 | **0.092884** | **0.954823** |
| **Signal transduction** | | | | | |
| A0A1X7VAN2 | Calmodulin | 3 | **0.004717** | **6.59E-07** | **0.090423** |
| A0A1X7UI48 | Histidine-tRNA ligase | 1 | **0.024449** | **5.24E-06** | 0.182332 |
| A0A1X7VIG0 | ADP-ribosylation factor 6 (Arf family) | 1 | 0.318505 | **0.054828** | 0.683634 |
| **Protein translation** | | | | | |
| A0A1X7VB92 | Aspartate-tRNA ligase, cytoplasmic | 1 | **0.047777** | **0.009516** | 0.303402 |
| A0A1X7V8E5 | Uncharacterized (Universal ribosomal protein S8 family) | 1 | 1 | **0.000838** | 0.244596 |
| A0A1X7V0I1 | Ubiquitin - 60S ribosomal protein L40 | 6 | **0.023366** | **0.008763** | 0.090423 |
| **Protein catabolism** | | | | | |
| A0A1X7VN30 | Proteasome subunit beta | 2 | **0.061227** | **0.001937** | **0.090423** |
| A0A1X7VGM8 | Palmitoyl-protein hydrolase 1 | 1 | **0.089645** | 0.680671 | 1 |
| A0A1X7VV07 | Sulfatase domain-containing protein ($Ca^{2+}$ Cofactor) | 1 | **0.003762** | **5.24E-06** | **0.090423** |

*Table continues next page

| Uniprot Accession number | Protein annotation | Proteins in cluster | 26ºC vs 28ºC | 26ºC vs 30ºC | 28ºC vs 30ºC |
|---|---|---|---|---|---|
| **Metabolic process** | | | | | |
| A0A1X7VEB3 | Adenosylhomocysteinase ($NAD^+$ cofactor) | 1 | **0.089645** | **0.000314** | **0.016798** |
| **Others** | | | | | |
| A0A1X7SVR6 | Uncharacterized | 4 | **3.53E-06** | **5.24E-06** | 0.40943 |
| A0A1X7VMX7 | Septin-type G domain containing protein | 1 | 0.831446 | **0.001133** | 0.576949 |
| A0A1X7SMT9 | Uncharacterized | 1 | **0.066834** | **0.012566** | 1 |
| A0A1X7VLW9 | Transket_pyr domain-containing protein ($Co^{2+}$ and $Mg^{2+}$ cofactor) | 1 | 1 | **0.055495** | 0.40943 |
| A0A1X7V015 | DUF3504 domain-containing protein | 1 | 1 | **0.040336** | 0.269237 |
| A0A1X7SJZ1 | Uncharacterized | 3 | 1 | **0.054828** | 0.683634 |
| A0A1X7SYB4 | Uncharacterized | 1 | 0.398718 | **0.054828** | **0.153691** |
| A0A1X7U869 | Store-operated calcium entry-associated regulatory factor | 1 | 1 | **0.054143** | 0.393734 |
| A0A1X7VNC8 | Uncharacterized (RNA helicase family) | 1 | 1 | **0.042849** | 0.116539 |
| A0A1X7T7Q1 | Uncharacterized | 2 | 0.24654 | **0.049142** | 0.393734 |

**Table S3.** Protein cluster report including identification probabilities, sequence coverage, and numbers of unique peptides and spectra.

Click here to download Table S3